

Investigation of magnetic properties and microwave characteristics of obliquely sputtered NiFe/MnIr bilayers

Nguyen N. Phuoc, Wee Tee Soh, Guozhi Chai, and C. K. Ong

Citation: *J. Appl. Phys.* **113**, 073902 (2013); doi: 10.1063/1.4792496

View online: <http://dx.doi.org/10.1063/1.4792496>

View Table of Contents: <http://jap.aip.org/resource/1/JAPIAU/v113/i7>

Published by the [American Institute of Physics](#).

Additional information on J. Appl. Phys.

Journal Homepage: <http://jap.aip.org/>

Journal Information: http://jap.aip.org/about/about_the_journal

Top downloads: http://jap.aip.org/features/most_downloaded

Information for Authors: <http://jap.aip.org/authors>

ADVERTISEMENT



AIPAdvances

Now Indexed in Thomson Reuters Databases

Explore AIP's open access journal:

- Rapid publication
- Article-level metrics
- Post-publication rating and commenting

Investigation of magnetic properties and microwave characteristics of obliquely sputtered NiFe/MnIr bilayers

Nguyen N. Phuoc,^{1,a)} Wee Tee Soh,² Guozhi Chai,¹ and C. K. Ong²

¹Temasek Laboratories, National University of Singapore, 5A Engineering Drive 2, Singapore 117411

²Center for Superconducting and Magnetic Materials, Department of Physics, National University of Singapore, 2 Science Drive 3, Singapore 117542

(Received 20 December 2012; accepted 1 February 2013; published online 15 February 2013)

A comprehensive investigation of the magnetic properties and high frequency characteristics of NiFe/MnIr bilayers with regards to oblique deposition angle was conducted in conjunction with an analysis based on the Landau-Lifshitz-Gilbert equation. It was found that exchange bias can be significantly enhanced with the variation of oblique deposition angle, which is interpreted in terms of the formation of inclined columnar structure of the films often observed in samples fabricated by this oblique deposition technique. Moreover, the uniaxial magnetic anisotropy field and the resonance frequency are increased with the increasing of oblique deposition angle. The variations of effective Gilbert damping factor and the frequency linewidth with oblique deposition angle are also presented and discussed in details. © 2013 American Institute of Physics. [<http://dx.doi.org/10.1063/1.4792496>]

I. INTRODUCTION

Among various research themes in magnetism, exchange bias stands as one of the most interesting topics that have been received much attention from many researchers.^{1–3} This effect refers to the shift of the hysteresis loops in materials having ferromagnetic (FM)/antiferromagnetic (AF) interfaces when they undergo a field cooling procedure from a temperature higher than the Néel point or when they are fabricated under an applied magnetic field.^{1–3} Although extensively studied due to its extensive application in magnetic recording industry^{4–7} as well as potential applications in microwave devices,^{8–16} the physical origin of this intriguing phenomenon together with some associated effect is still in controversy and needs further research to elucidate. In the literature, exchange bias has been investigated with respect to many influence factors such as thickness dependence,^{1,8,11,12,14–16} temperature dependence,^{1,6,16–18} microstructure dependence,^{1,3,18–20} and fabrication condition dependence^{20,21} of this effect. However, it appears that there is a lacking of research that focuses on the influence of oblique deposition in exchange-biased thin films.^{22–24} In this work, we therefore aim to study the effect of oblique deposition on magnetic and microwave properties of exchange-biased NiFe/MnIr bilayers. This study in the sense of fundamental research may assist us to have an insight of exchange bias. Besides, from application perspective, our research work has a great implication for high frequency application based on magnetic thin films because both exchange bias^{8–15} and oblique deposition^{25–30} are proven to be effective ways to tune the ferromagnetic resonance frequency. Hence, it may be interesting to investigate the possibility of combining these two ways together to push the resonance frequency to even higher range. With these objectives in mind, we carry out in the present research work, a

detailed investigation to see how the oblique deposition angle affects both the static magnetic properties in the hysteresis loops and the dynamic magnetization in the permeability spectra of the exchange-biased NiFe/MnIr bilayers and discuss the results in light of the analysis based on the Landau-Lifshitz-Gilbert (LLG) equation.

II. EXPERIMENT

Thin films of NiFe (125 nm)/MnIr (15 nm) bilayers were fabricated onto Si (100) substrates at room temperature using a radio-frequency (RF) magnetron sputter-deposition system with the base pressure of 7×10^{-7} Torr. The targets used in this fabrication are Ni₈₀Fe₂₀ and Mn₇₅Ir₂₅ alloy targets. A capping layer of SiO₂ with the thickness of 10 nm was deposited on the top of the samples to protect them from oxidation. The argon pressure was kept at 10^{-3} Torr during the deposition process by introducing argon gas at the flow rate of 16 SCCM (SCCM denotes cubic centimeter per minute at STP). The deposition setup is shown in Fig. 1, where the substrates were put at an oblique angle ranging from 0° to 45°. With this arrangement, the easy axis of the present films induced by oblique deposition is perpendicular to incident plane. A magnetic field of about 200 Oe was applied during the deposition process along the easy axis induced by oblique deposition in order to assist the inducement of magnetic anisotropy. The composition was determined by energy dispersive X-ray spectroscopy (EDS) and the thickness of each layer was controlled both by the deposition time and by keeping the deposition rate constant, which was verified by a thickness profile meter. For the structural properties of the films, an X-ray diffractometer using CuK α radiation was employed to characterize. A vibrating sample magnetometer (VSM) was used for the measurement of magnetization curves at room temperature. The permeability spectra over the frequency range from 0.05 GHz to 5 GHz were obtained by a shorted micro-strip transmission-line perturbation method³¹ using a fixture developed in our laboratory.

^{a)}Author to whom correspondence should be addressed. Electronic mail: tslnnp@nus.edu.sg. Tel.: 65-65162816. Fax: 65-67776126.

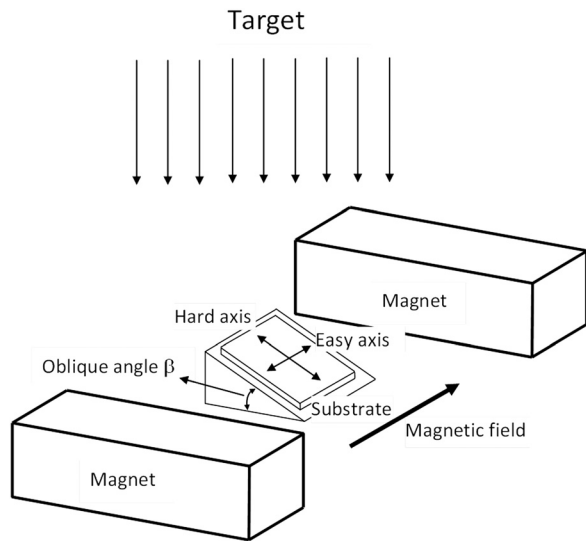


FIG. 1. Schematic view of the present oblique deposition system.

III. RESULTS AND DISCUSSION

Figure 2 presents X-ray diffraction patterns for a series of our NiFe/MnIr bilayer samples with oblique deposition angle changed from 0° to 45° . There are two prominent peaks observed which corresponds to the MnIr fcc (111)

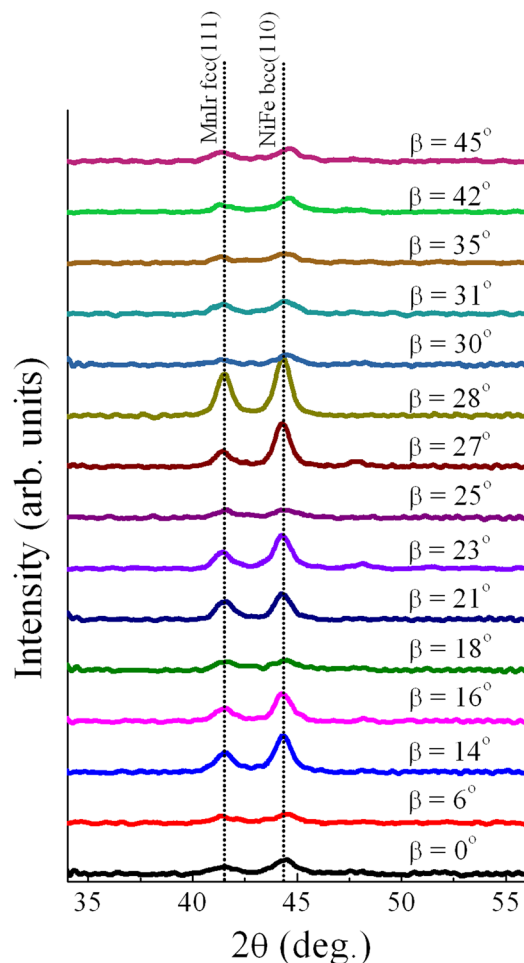


FIG. 2. XRD profiles of NiFe-MnIr bilayered films grown at various oblique deposition angles.

peak and NiFe bcc (110) peak. It can be seen that as the oblique deposition angle is increased, especially in the range from 30° to 45° , the NiFe bcc (110) peak is moved to the higher diffraction angle whereas the MnIr fcc (111) peak position is practically unchanged. This unambiguously indicates that there is a contraction in the lattice spacing of NiFe bcc (110). The contraction of NiFe bcc (110) lattice spacing can be interpreted in terms of the formation of the columnar grains which are tilted due to the self-shadow effect^{25–30,32–34} of the oblique deposition method. As the oblique angle is increased, the tilting of the columnar grains is increased leading to some distortion of the lattice of the films in such a way that the lattice spacing is reduced substantially.^{24,25}

Shown in Fig. 3 are several representative hysteresis loops of NiFe/MnIr bilayer films with different oblique deposition angles measured at room temperature along the easy axis and the hard axis. Here, the easy axis is the one in the same direction as the magnetic field applied during deposition. The hard axis is the one that is perpendicular to the deposition magnetic field but it is still lying in the plane of the film.^{12,13} A detailed description for the definition of the easy axis and hard axis is provided in Fig. 1. It can be seen clearly in Fig. 3 that all the easy axis loops are shifted to the negative direction which is indicative of the presence of exchange bias coupling between the FM (NiFe) and AF (MnIr) layers. The hard axis magnetization curves show typical slanted loops implying that there is also an uniaxial magnetic anisotropy present in these films. More interesting, one can observe that the hard axis loops become more slanted as the oblique deposition angle is increased. This behavior suggests

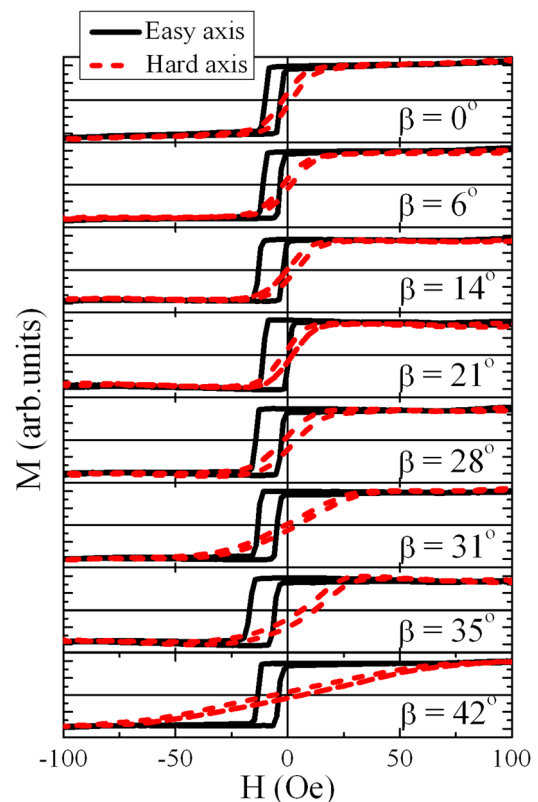


FIG. 3. Representative hysteresis loops measured along easy axis and hard axis at room temperature for different NiFe-MnIr films grown at various oblique deposition angles.

that the magnetic anisotropy is increased with increasing of the oblique deposition angle. More quantitative discussion on this behavior together with the contribution of each separated magnetic anisotropy will be given later.

Now we focus on the measurement of dynamic magnetic characteristics of these films. The permeability spectra of the films measured at room temperature for some representative oblique angles are revealed in Fig. 4 with both real and imaginary parts. As demonstrated in Fig. 4(b), the peak in the imaginary permeability spectra is found to be shifted toward higher frequency range when the oblique deposition angle is increased. This behavior unambiguously indicates that the ferromagnetic resonance frequency is increased with the increasing of oblique deposition angle. For a more quantitative analysis of these dynamic magnetic properties, the LLG

equation³⁵ as below is employed to fit the experimental dynamic permeability spectra,

$$\frac{d\vec{M}}{dt} = -\gamma(\vec{M} \times \vec{H}) + \frac{\alpha_{eff}}{M} \vec{M} \times \frac{d\vec{M}}{dt}. \quad (1)$$

Here, M represents the magnetization of the films, H is the magnetic field, α_{eff} is the dimensionless effective Gilbert damping coefficient (α_{eff} includes intrinsic and several extrinsic sources of damping^{8,15,23}), and γ is the gyromagnetic ratio. By solving the LLG equation with the assumption of macrospin approximation and the presence of only in-plane uniaxial anisotropy in the films, one can obtain the expression of the real and imaginary parts of permeability spectra as follows:^{27,28}

$$\mu' = 1 + 4\pi M_S \gamma^2 \frac{(4\pi M_S + H_K^{dyn})(1 + \alpha_{eff}^2)[\omega_R^2(1 + \alpha_{eff}^2) - \omega^2] + (4\pi M_S + 2H_K^{dyn})(\alpha_{eff}\omega)^2}{[\omega_R^2(1 + \alpha_{eff}^2) - \omega^2]^2 + [\alpha_{eff}\omega\gamma(4\pi M_S + 2H_K^{dyn})]^2}, \quad (2)$$

$$\mu'' = 4\pi M_{eff} \gamma \omega \alpha_{eff} \frac{\gamma^2(4\pi M_{eff} + H_K^{dyn})^2(1 + \alpha_{eff}^2) + \omega^2}{[\omega_R^2(1 + \alpha_{eff}^2) - \omega^2]^2 + [\alpha_{eff}\omega\gamma(4\pi M_{eff} + 2H_K^{dyn})]^2}. \quad (3)$$

Here, γ , M_S , H_K^{dyn} , and ω_R ($\omega_R = 2\pi f_{FMR}$) are the gyromagnetic ratio, the saturation magnetization, dynamic magnetic anisotropy, and ferromagnetic resonance frequency, respectively. The saturation magnetization $4\pi M_S$ can be obtained from VSM measurement which is 10 kG while the dynamic magnetic anisotropy field H_K^{dyn} and the effective Gilbert damping α_{eff} can be considered as fitting parameters. Based on the above Eqs. (2)

and (3), we can fit the experimental data very well with the theoretical curves, which are represented as the lines in Fig. 4.

Figure 5 provide a summary of the dependences of the exchange bias field H_E , the coercivity measured along the

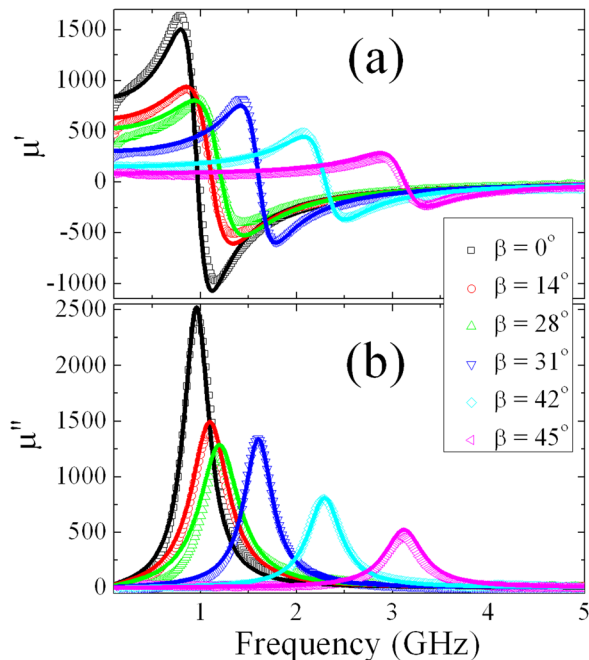


FIG. 4. Representative permeability spectra of NiFe-MnIr films grown at various oblique deposition angles. (a) Real part μ' . (b) Imaginary part μ'' . Lines are fitted from LLG equation.

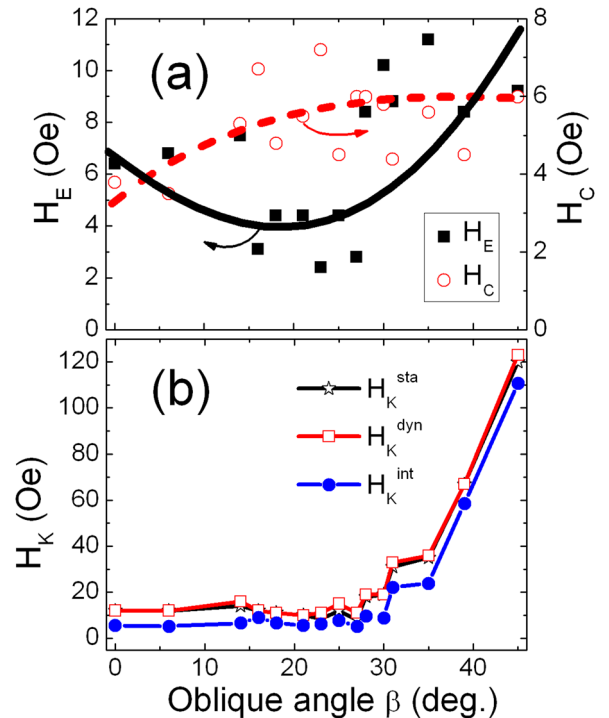


FIG. 5. (a) Variations of exchange bias field (H_E) and coercivity (H_C) along the easy axis as a function of oblique deposition angle. Lines are served as a guide to the eyes. (b) Variations of intrinsic uniaxial (H_K^{int}), static (H_K^{sta}), and dynamic (H_K^{dyn}) magnetic anisotropy fields as functions of oblique deposition angle.

easy axis (H_C), the static magnetic anisotropy field H_K^{sta} , the dynamic magnetic anisotropy field H_K^{dyn} , and the intrinsic uniaxial magnetic anisotropy field H_K^{int} . The exchange bias field H_E is defined as the shift of the center of the magnetization curve along the easy axis whereas the static magnetic anisotropy field H_K^{sta} is determined from the slope of the hard axis hysteresis loop.^{10,12,15,36,37} It is noted that this static magnetic anisotropy field H_K^{sta} is the total effective static magnetic anisotropy field and is the sum of the unidirectional anisotropy field (which is exchange bias field H_E) and the intrinsic uniaxial magnetic anisotropy field H_K^{int} ($H_K^{\text{sta}} = H_E + H_K^{\text{int}}$).^{36,37} In addition, one should note that the easy axis of H_K^{sta} is not changed with the increasing of oblique angle and it is in the same direction as the direction of the unidirectional anisotropy defined by the magnetic field applied during deposition. Hence, we can obtain H_K^{int} by subtraction of H_E from H_K^{sta} ($H_K^{\text{int}} = H_K^{\text{sta}} - H_E$).^{36,37} The dynamic magnetic anisotropy field H_K^{dyn} , on the other hand, is obtained from the LLG fitting procedure as mentioned above. As observed in Fig. 5(a), exchange bias field is generally increased with oblique angle except a slight decrease in the range from 16° to 23° . This behavior may possibly be due to the above-mentioned self-shadow effect which results in a formation of tilted columnar structure leading to some distortion of the lattice of the films.^{25–30} This distortion may assist in creating more pinning sites at the FM/AF interfaces which are important for emergence of the frozen AF spins accounting for exchange bias thus accounting for the enhancement of exchange bias with oblique angle as observed.²⁴ Also presented in Fig. 5(a) is the variation of the coercivity H_C with oblique deposition angle showing a slight increase of H_C with oblique angle. The mechanism of H_C is rather complicated, which is dependent not only on the value of the magnetic anisotropy but also on the reversal modes of the magnetization process. As the magnetic anisotropy is hugely changed while the coercivity is practically unchanged, one may tentatively draw a conclusion that the coercivity in this case is governed mostly by the reversal modes rather than by the magnitude of the magnetic anisotropy. We argue that it is also because the self-shadow effect that causes the intrinsic uniaxial anisotropy field H_K^{int} increased with the increasing of the oblique deposition angle as seen in Fig. 5(b). This behavior was quite well established in the literature with many similar observations in various systems of single layered FM.^{25–30} Due to the increasing of both exchange bias field H_E and the uniaxial anisotropy field H_K^{int} with the oblique deposition angle, the total effective static magnetic anisotropy field H_K^{sta} is increased accordingly. However, it should be noted that this increment is mostly due to the contribution of H_K^{int} explaining why the trends of H_K^{sta} and H_K^{int} with oblique deposition angle are quite similar. For example, when the oblique deposition angle is changed from 0° to 45° , H_K^{int} is increased from 6 Oe to a high value up to 110 Oe while H_E is only changed from 6 Oe to 9 Oe. The reason for these different behaviors lies in the fact that the self-shadow effect resulting in a formation of tilted columnar structure in oblique deposition governs H_K^{int} and H_E in different ways. While this tilted columnar structure containing elongated grains may lead to the emergence

of shape anisotropy and magnetocrystalline anisotropy causing a great enhancement of H_K ,^{23,25–30} it may just only create more pinning sites at the FM/AF interfaces, thereby leading to a moderate increment in H_E . Also as observed in Fig. 5(b), the difference between dynamic magnetic anisotropy field H_K^{dyn} obtained from LLG fitting and the static magnetic anisotropy field H_K^{sta} estimated from M-H loops is negligible suggesting that there is practically no rotational anisotropy field present in these series of samples^{15,17,36,37}

According to Kittel,³⁸ the ferromagnetic resonance frequency f_{FMR} and the dynamic magnetic anisotropy field H_K^{dyn} can be related to each other through the following equation:

$$f_{\text{FMR}} = \frac{\gamma}{2\pi} \sqrt{H_K^{\text{dyn}}(H_K^{\text{dyn}} + 4\pi M_S)}. \quad (4)$$

Since H_K^{dyn} is increased with the increasing of oblique deposition angle as discussed above and the saturation magnetization M_S is constant for all the samples, the ferromagnetic resonance frequency f_{FMR} is increased with oblique deposition angle accordingly as in Fig. 6(a). This characteristic has an important implication from the application perspective. By combining both exchange bias and oblique deposition technique, we can tune the resonance frequency from 0.9 GHz up to 3.2 GHz. The static permeability μ_S , however, is reduced when the oblique deposition angle is increased as observed in Fig. 6(b). This reduction can be interpreted based on the following equation which reveals the relationship between the static permeability μ_S and the effective static magnetic anisotropy H_K^{sta} ,¹¹

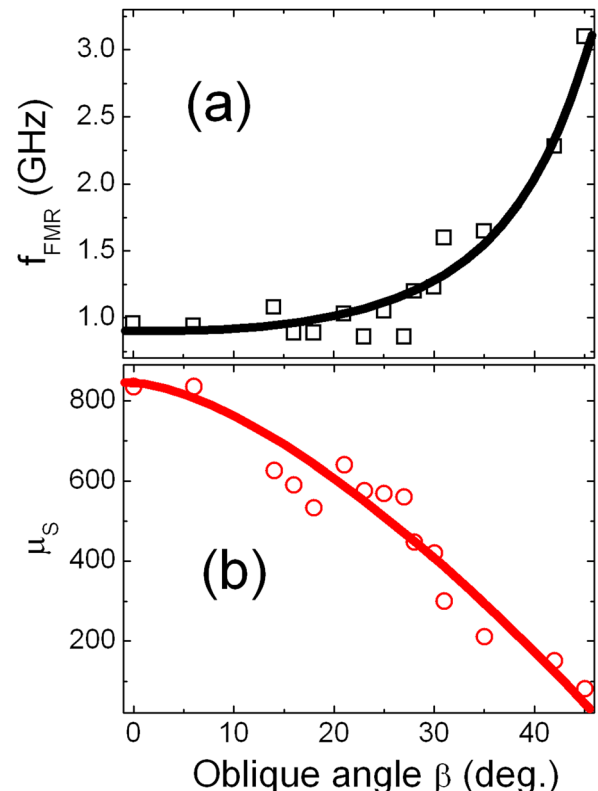


FIG. 6. Dependences of (a) ferromagnetic resonance frequency (f_{FMR}), (b) static permeability (μ_S) with oblique deposition angle.

$$\mu_S = 1 + \frac{4\pi M_S}{H_K^{sta}}. \quad (5)$$

From the above formula, it can be easily deduced that as H_K^{sta} is increased with oblique deposition angle as in Fig. 5(b) while M_S is constant, μ_S is expected to decrease when the oblique deposition angle increases.

Figure 7 summarizes the variations of the effective Gilbert damping coefficient α_{eff} and the frequency linewidth Δf with oblique deposition angle. It is interesting to observe that the variation trend of α_{eff} with oblique deposition angle as in Fig. 7(a) is roughly inverse to the trend of the dependence of exchange bias H_E with oblique angle as in Fig. 5(a). In particular, when the oblique angle is increased from 0° to around 25° , exchange bias field H_E is reduced while the effective Gilbert damping coefficient α_{eff} is increased. Then as the oblique angle increases from 25° to around 45° , the exchange bias H_E is increased whereas the effective Gilbert damping coefficient α_{eff} is now decreased. In order to interpret these seemingly interesting contradicted trends, one should be reminded that the effective Gilbert damping factor measured in our case consists of two main contribution: one is intrinsic and the other is extrinsic.^{8,11,15,23} While the intrinsic contribution solely comes from the material nature, the extrinsic one stems from various sources such as magnetic anisotropy dispersion, material inhomogeneity, two-magnon scattering due to defects, grain size variation, surface roughness etc.^{8,11,15,23} Since the materials for these series of samples are the same, one may naturally expect that the intrinsic contribution may not change with the oblique deposition angle. Hence, the variation of α_{eff} as in Fig. 7(a) is most likely due to the extrinsic contribution. Separating

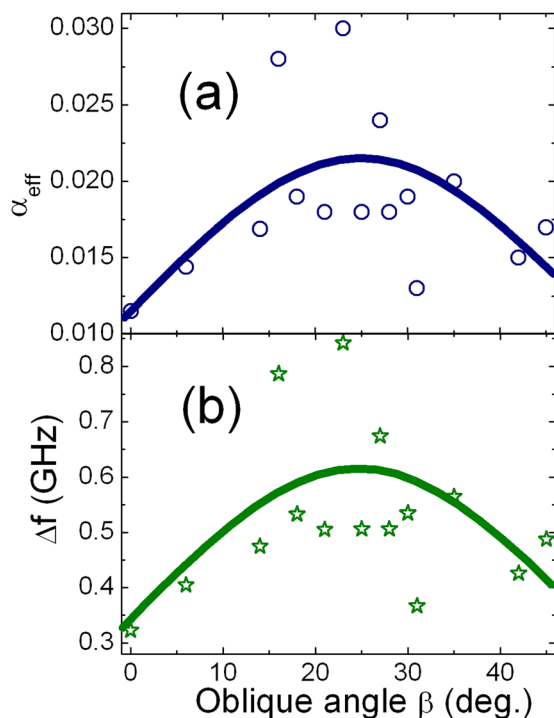


FIG. 7. Variations of (a) effective Gilbert damping factor (α_{eff}), and (b) frequency linewidth (Δf) on oblique deposition angle. Lines are served as a guide to the eyes.

the originating sources of the extrinsic contribution is quite complicated and beyond the scope of the present paper. However, in view of the contradicted variation trend of the effective Gilbert damping coefficient α_{eff} in Fig. 7(a) and the exchange bias field H_E in Fig. 5(a), we may tentatively attribute the variation of α_{eff} to the magnetic anisotropy dispersion as one of the main contribution. As the role of exchange bias interaction between FM and AF spins is to keep the FM spins well aligned into a defined direction, when this exchange bias surface energy increases (which manifests itself as the increasing of exchange bias field H_E) the FM spins will be better aligned along the easy axis, leading to the decreasing of magnetic anisotropy dispersion. The decreasing of magnetic anisotropy dispersion then brings about the reduction of the extrinsic damping. This explains why α_{eff} is decreased when H_E is increased and vice versa. Apparently, other extrinsic contributions such as two-magnon scattering, material inhomogeneity should not be ruled out and further studies where each contribution can be separated need to be performed to verify our argument.

It is well known that the frequency linewidth Δf is related to the effective Gilbert damping coefficient α_{eff} through the following formula:^{15,17}

$$\Delta f = \frac{\gamma \alpha_{eff} (4\pi M_S + 2H_K^{dyn})}{2\pi}. \quad (6)$$

Since M_S is not changed with the variation of oblique deposition angle and is also because $4\pi M_S$ is much larger than H_K^{dyn} , the change of Δf is mostly due to the variation of α_{eff} . This explains why the behavior of Δf with oblique angle as in Fig. 7(b) is quite similar to the variation of α_{eff} in Fig. 7(a).

IV. SUMMARY AND CONCLUSION

To summarize, we have performed a detailed investigation of the influence of oblique deposition angle on the magnetic and microwave properties of NiFe/MnIr exchange-biased bilayers. It was found that oblique deposition can tailor the magnitude of exchange bias significantly which is suggested to be due to the formation of tilted columnar structure arising from a self-shadow effect in oblique deposited films. We also found that the uniaxial anisotropy field was significantly increased with oblique deposition angle due to this inclined columnar structure. As a result, the ferromagnetic resonance frequency is increased with oblique deposition angle, which implies that exchange bias and oblique deposition technique can be combined together to push the resonance frequency to higher range. In our case, the resonance frequency can be pushed up to 3 GHz, which is quite promising for microwave applications. Our study also revealed that the effective Gilbert damping coefficient is strongly dependent on the oblique deposition angle, which is ascribed mainly to the dispersion of magnetic anisotropy.

ACKNOWLEDGMENTS

The financial support from the Defence Research and Technology Office (DRTech) of Singapore is gratefully acknowledged.

- ¹J. Nogués and I. K. Schuller, *J. Magn. Magn. Mater.* **192**, 203 (1999).
- ²R. L. Stamps, *J. Phys. D: Appl. Phys.* **33**, R247 (2000).
- ³J. Nogués, J. Sort, V. Langlais, V. Skumryev, S. Suriñach, J. S. Muñoz, and M. D. Baró, *Phys. Rep.* **422**, 65 (2005).
- ⁴B. Dieny, V. S. Speriosu, S. S. P. Parkin, B. A. Gurney, D. R. Wilhoit, and D. Mauri, *Phys. Rev. B* **43**, 1297 (1991).
- ⁵C. Chappert, A. Fert, and F. N. Van Dau, *Nature Mater.* **6**, 813 (2007).
- ⁶N. N. Phuoc and T. Suzuki, *J. Appl. Phys.* **101**, 09E501 (2007).
- ⁷F. Radu, R. Abrudan, I. Radu, D. Schmitz, and H. Zabel, *Nat. Commun.* **3**, 715 (2012).
- ⁸B. K. Kuanr, R. E. Camley, and Z. Celinski, *J. Appl. Phys.* **93**, 7723 (2003).
- ⁹S. Queste, S. Dubourg, O. Acher, K. U. Barholz, and R. Mattheis, *J. Appl. Phys.* **95**, 6873 (2004).
- ¹⁰Y. Lamy, B. Viala, and I. L. Prejbeanu, *IEEE Trans. Magn.* **41**, 3517 (2005).
- ¹¹D. Spenato, S. P. Pogossian, D. T. Dekadjevi, and J. Ben Youssef, *J. Phys. D: Appl. Phys.* **40**, 3306 (2007).
- ¹²N. N. Phuoc, S. L. Lim, F. Xu, Y. G. Ma, and C. K. Ong, *J. Appl. Phys.* **104**, 093708 (2008).
- ¹³N. N. Phuoc, F. Xu, and C. K. Ong, *Appl. Phys. Lett.* **94**, 092505 (2009).
- ¹⁴C. Jiang, D. Xue, and W. Sui, *Thin Solid Films* **519**, 2527 (2011).
- ¹⁵N. N. Phuoc and C. K. Ong, *Physica B* **406**, 3514 (2011).
- ¹⁶K. O'Grady, L. E. Fernandez-Outon, and G. Vallejo-Fernandez, *J. Magn. Magn. Mater.* **322**, 883 (2010).
- ¹⁷H. Y. Chen, N. N. Phuoc, and C. K. Ong, *J. Appl. Phys.* **112**, 053920 (2012).
- ¹⁸K. Imakita, M. Tsunoda, and M. Tahahashi, *Appl. Phys. Lett.* **85**, 3812 (2004).
- ¹⁹J. Wang, W. Kuch, L. I. Chelaru, F. Offi, and M. Kotsugi, *Appl. Phys. Lett.* **86**, 122504 (2005).
- ²⁰N. N. Phuoc and T. Suzuki, *Phys. Status Solidi C* **4**, 4380 (2007).
- ²¹M. Mao, C. Cerjan, B. Law, F. Grabner, and S. Vaidya, *J. Appl. Phys.* **87**, 4933 (2000).
- ²²B. Diouf, L. Gabillet, A. R. Fert, D. Hrabovsky, V. Prochazka, E. Snoeck, and J. F. Bobo, *J. Magn. Magn. Mater.* **265**, 204 (2003).
- ²³R. L. Rodríguez-Suárez, L. H. Vilela-Leão, T. Bueno, A. B. Oliveira, J. R. L. de Almeida, P. Landeros, S. M. Rezende, and A. Azevedo, *Phys. Rev. B* **83**, 224418 (2011).
- ²⁴N. N. Phuoc, G. Chai, and C. K. Ong, *J. Appl. Phys.* **112**, 113908 (2012).
- ²⁵E. Yu, J. S. Shim, I. Kim, J. Kim, S. H. Han, H. J. Kim, K. H. Kim, and M. Yamaguchi, *IEEE Trans. Magn.* **41**, 3259 (2005).
- ²⁶X. Fan, D. Xue, M. Lin, Z. Zhang, D. Guo, C. Jiang, and J. Wei, *Appl. Phys. Lett.* **92**, 222505 (2008).
- ²⁷N. N. Phuoc, F. Xu, and C. K. Ong, *J. Appl. Phys.* **105**, 113926 (2009).
- ²⁸Z. Zhang, X. Fan, M. Lin, D. Guo, G. Chai, and D. Xue, *J. Phys. D: Appl. Phys.* **43**, 085002 (2010).
- ²⁹I. Barsukov, P. Landeros, R. Meckenstock, J. Lindner, D. Spoddig, Z. A. Li, B. Krumme, H. Wend, D. L. Mills, and F. Farle, *Phys. Rev. B* **85**, 014420 (2012).
- ³⁰G. Wang, C. Dong, W. Wang, Z. Wang, G. Chai, C. Jiang, and D. Xue, *J. Appl. Phys.* **112**, 093907 (2012).
- ³¹Y. Liu, L. F. Chen, C. Y. Tan, H. J. Liu, and C. K. Ong, *Rev. Sci. Instrum.* **76**, 063911 (2005).
- ³²T. G. Knorr and R. W. Hoffman, *Phys. Rev.* **113**, 1039 (1959).
- ³³R. D. McMichael, C. G. Lee, J. E. Bonevich, P. J. Chen, W. Miller, and W. F. Egelhoff, Jr., *J. Appl. Phys.* **88**, 3561 (2000).
- ³⁴F. Tang, D. L. Liu, D. X. Ye, Y. P. Zhao, T. M. Lu, G. C. Wang, and A. Vijayaraghavan, *J. Appl. Phys.* **93**, 4194 (2003).
- ³⁵T. L. Gilbert, *IEEE Trans. Magn.* **40**, 3443 (2004).
- ³⁶J. McCord, R. Mattheis, and D. Elefant, *Phys. Rev. B* **70**, 094420 (2004).
- ³⁷J. McCord, R. Kaltofen, T. Gemming, R. Huhne, and L. Schultz, *Phys. Rev. B* **75**, 134418 (2007).
- ³⁸C. Kittel, *Phys. Rev.* **71**, 270 (1947).